Current Biology *16*, 854–862, May 9, 2006 DOI 10.1016/j.cub.2006.03.083

Article

MIG-10/Lamellipodin and AGE-1/PI3K Promote Axon Guidance and Outgrowth in Response to Slit and Netrin

Chieh Chang,[1,2,3,6] Carolyn E. Adler,[1,2] Matthias Krause,[4,7] Scott G. Clark,[5] Frank B. Gertler,[4] Marc Tessier-Lavigne,[3,8,*] and Cornelia I. Bargmann[1,2,*]

[1] Howard Hughes Medical Institute
The Rockefeller University
1230 York Avenue
New York, New York 10021

[2] Department of Anatomy
Howard Hughes Medical Institute
University of California, San Francisco
San Francisco, California 94143

[3] Department of Biological Sciences
Howard Hughes Medical Institute
Stanford University
Stanford, California 94305

[4] Department of Biology and Center for Cancer Research
Massachusetts Institute of Technology
Cambridge, Massachusetts 02139

[5] Molecular Neurobiology Program
Department of Pharmacology
Skirball Institute
New York University School of Medicine
New York, New York 10016

Summary

Background: The cytoplasmic *C. elegans* protein MIG-10 affects cell migrations and is related to mammalian proteins that bind phospholipids and Ena/VASP actin regulators. In cultured cells, mammalian MIG-10 promotes lamellipodial growth and Ena/VASP proteins induce filopodia.

Results: We show here that during neuronal development, *mig-10* and the *C. elegans* Ena/VASP homolog *unc-34* cooperate to guide axons toward UNC-6 (netrin) and away from SLT-1 (Slit). The single mutants have relatively mild phenotypes, but *mig-10; unc-34* double mutants arrest early in development with severe axon guidance defects. In axons that are guided toward ventral netrin, *unc-34* is required for the formation of filopodia and *mig-10* increases the number of filopodia. In *unc-34* mutants, developing axons that lack filopodia are still guided to netrin through lamellipodial growth. In addition to its role in axon guidance, *mig-10* stimulates netrin-dependent axon outgrowth in a process that requires the *age-1* phosphoinositide-3 lipid kinase but not *unc-34.*

Conclusions: *mig-10* and *unc-34* organize intracellular responses to both attractive and repulsive axon guidance cues. *mig-10* and *age-1* lipid signaling promote axon outgrowth; *unc-34* and to a lesser extent *mig-10* promote filopodia formation. Surprisingly, filopodia are largely dispensable for accurate axon guidance.

*Correspondence: marctl@gene.com (M.T.-L.); cori@rockefeller.edu (C.I.B.)

[6] Present address: Department of Biology, McGill University, Montreal, Quebec H3A 1B1, Canada.

[7] Present address: Randall Division of Cell & Molecular Biophysics, King's College London, London SE1 1UL, United Kingdom.

[8] Present address: Genentech, Inc., 1 DNA Way, South San Francisco, California 94080.

Introduction

During neuronal development, the neuronal growth cone responds to conserved extracellular guidance cues with cytoskeletal rearrangements and directed cell movements [1–7]. In a typical growth cone, finger-like filopodia with bundled actin filaments extend from a lamellipodial region with loosely crosslinked actin webs [4]. In both neuronal and nonneuronal filopodia, the Ena/VASP family of actin regulators promote the formation of long unbranched actin filaments by protecting actin barbed ends from capping proteins [5, 8–13]. Genetic and biochemical results suggest that Ena/VASP proteins have important roles in guidance to the conserved axon guidance factor UNC-6/netrin via its receptor UNC-40/DCC [7, 13]. UNC-34/Ena also functions in repulsive axon guidance downstream of the Slit receptor Robo at the *Drosophila* midline and in *C. elegans* AVM axons, and in repulsive axon guidance downstream of the netrin receptor UNC-5 in motor neurons [5, 11, 14].

Members of the Ena/VASP family share a conserved domain structure with an Ena/VASP homology 1 (EVH1) domain, a proline-rich region, and an Ena/VASP homology 2 (EVH2) domain [15–18]. The EVH1 domain binds a consensus FPPPP proline-rich motif that is present in focal adhesion proteins and in the guidance receptor Robo [5, 15, 16] and in the cytoplasmic protein Lamellipodin (Lpd) [19]. Lpd colocalizes with Ena/VASP in fibroblast lamellipodia and filopodia and in neuronal growth cones, and Lpd stimulates F-actin formation during fibroblast lamellipodial protrusion. A Lpd-related molecule, RIAM, stimulates integrin-dependent actin polymerization, lamellipodia formation, and cell spreading in T cells [20]. Lpd and RIAM each have multiple FPPPP motifs, a Ras/Rap GTPase association domain, a lipid binding pleckstrin homology (PH) domain, and a profilin binding proline-rich domain (Figures 1A and 1B). The PH domain of Lpd binds PI(3,4)P2 (PIP2) phospholipids [19, 20].

The *C. elegans* genome encodes a single molecule homologous to mammalian Lpd and RIAM, MIG-10. *mig-10* mutants have disrupted embryonic cell migrations [21] that resemble those in animals mutant for *unc-34,* the sole *C. elegans* Ena/VASP ortholog [22]. We show here that *mig-10* has important functions in axon outgrowth and guidance that are masked by partial redundancy between *mig-10* and *unc-34* genes. Our results suggest that MIG-10 and UNC-34 have overlapping but distinct roles in organizing filopodial and lamellipodial growth in developing axons.

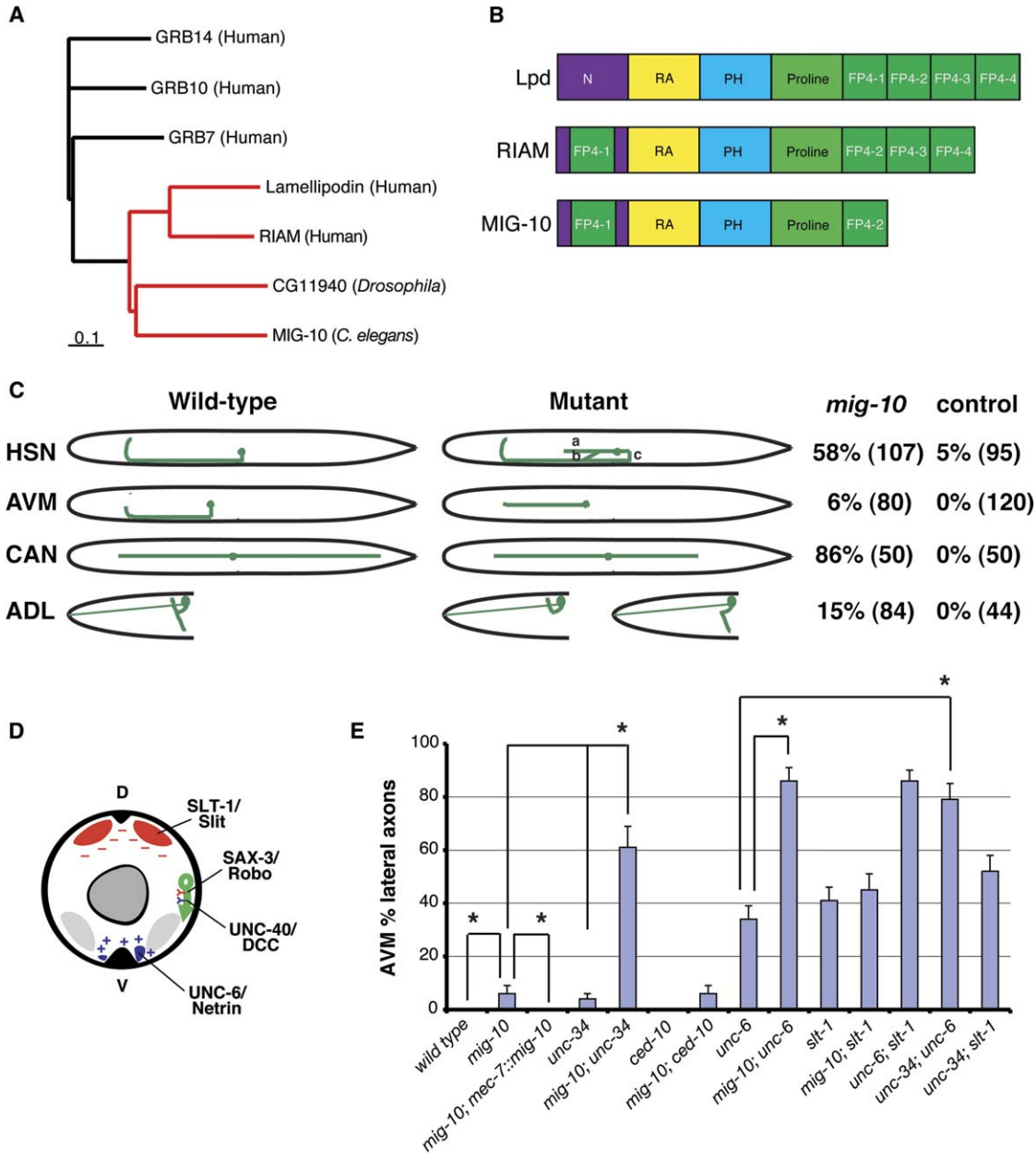

Figure 1. MIG-10/Lamellipodin Affects Axon Guidance

(A) Phylogram of the evolutionary relationships of *C. elegans* MIG-10 and its mammalian and *Drosophila* homologs. The horizontal distance represents the degree of sequence divergence, and the scale bar at the bottom corner corresponds to 10% substitution events.

(B) Schematic representation of domain organization of Lamellipodin, RIAM, and MIG-10. N, amino-terminal region; RA, Ras-association domain; PH, pleckstrin homology domain; Proline, proline-rich domain; FP4, motifs fitting the FPPPP consensus for EVH1 binding.

(C) Axon guidance defects in *mig-10* mutants. Left, schematic diagrams of wild-type and mutant axons. Right, percentage of defective neurons in *mig-10(ct41)* and controls. For HSN, most lateral axons grew either anteriorly (b) or posteriorly (c) before growing ventrally; only 10% failed to reach the ventral midline entirely (a). For AVM, only axons that failed to reach the ventral midline were scored. For CAN posterior axons, 66% extended between 50%–75% of their normal length, and 20% extended less than 50% of their normal length. For ADL, 8% of the cells lacked ventral branches and 7% lacked dorsal branches. Transgenes are described in Experimental Procedures. In parentheses are the number of animals or neurons scored.

(D) Cross-section showing cells and molecules that affect ventral guidance of AVM axon (green). Dorsal muscles express the repellent SLT-1/Slit (red). Ventral axons express the attractant UNC-6/netrin (purple).

(E) Quantitation of AVM axon guidance defects. All mutations represent the strongest available loss-of-function alleles. In all figures, error bars represent standard error of the proportion. Asterisks and brackets represent $p < 0.05$ by t test or Bonferroni t test (in the case of multiple comparisons).

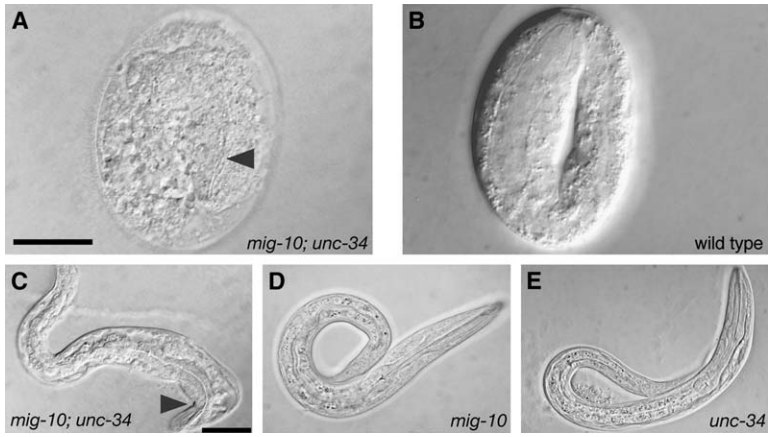

Figure 2. Synthetic Lethality of *mig-10* and *unc-34* Mutations

(A) Representative arrested midembryonic stage *mig-10; unc-34* double mutant with disorganized tissues. Arrowhead indicates partially differentiated pharynx.

(B) Wild-type 2-fold embryo.

(C) Representative arrested early L1 stage *mig-10; unc-34* double mutant. Arrowhead indicates head malformation.

(D and E) Viable *mig-10* (D) and *unc-34* (E) single mutants at L1 stage.

All panels are differential interference contrast (DIC) images. Scale bars equal 10 μm.

Results

MIG-10 Affects Netrin-Dependent and Slit-Dependent Axon Guidance

The *mig-10(ct41)* mutation leads to an early stop codon in all three known splice forms of *mig-10* and is a candidate null mutation [21]. We examined axon structure in these mutants by using a panel of transgenic lines expressing the green fluorescent protein (GFP) in different neurons. Many axons had mild guidance defects in *mig-10* mutants (Figure 1C). In HSN motor neurons, which are guided ventrally in response to netrin, about half of the axons of *mig-10* mutants had aberrant lateral or ventral-lateral trajectories. This result suggests that *mig-10* could play a role in netrin signaling in HSN (see below). A fraction of AVM mechanosensory neurons, which are guided ventrally by attraction to netrin and repulsion from Slit, were also defective in *mig-10* mutants. The branches of the ADL sensory neuron grow dorsally and ventrally in response to netrin and Slit [23]; both branches were occasionally lost in *mig-10* mutants. The posterior process of the bipolar CAN neuron, whose guidance cues are unknown, often terminated prematurely in *mig-10* mutants. HSN and CAN also have cell migration defects in *mig-10* mutants [21], but their axon defects cannot be explained purely as indirect effects of mismigration; both HSN axon defects and CAN axon defects are much more severe in *mig-10* mutants than they are in several other mutants in which cell migration is comparably abnormal [22]. Among other defects observed at low frequency were excessive midline crossing by the PVQ and PVP interneurons and defasciculation of the ventral nerve cord (data not shown). These defects suggest that *mig-10* contributes to many guidance decisions.

The AVM pioneer axon is easily visualized and convenient for detailed analysis of *C. elegans* axon guidance. To determine whether *mig-10* acts directly in migrating axons or indirectly in other cells, we expressed a *mig-10* cDNA under the control of a *mec-7* promoter, which is expressed strongly in six neurons including AVM [24]. A *mec-7::mig-10* transgene rescued the mild ventral guidance defect in AVM, suggesting that *mig-10* can act cell autonomously in developing neurons (Figure 1E).

The AVM axon is guided ventrally by attraction to UNC-6 (netrin) and repulsion from dorsal SLT-1 (Slit) (Figure 1D) [25–27]. Mutations in *unc-6*, its receptor *unc-40/DCC*, *slt-1*, or its receptor *sax-3/Robo* cause ventral guidance defects in 30%–40% of AVM axons; in double mutants in which both *unc-6* and *slt-1* pathways are inactivated, AVM ventral guidance fails completely. Thus, enhancement of an *unc-6(null)* mutant can identify genes that affect *slt-1*-dependent guidance in AVM, while enhancement of a *slt-1(null)* mutant can identify genes involved in *unc-6* signaling [11, 28]. *mig-10; unc-6* double mutants displayed strongly enhanced AVM guidance defects similar to those of *slt-1 unc-6* double mutants (Figure 1E). In contrast, *mig-10; slt-1* double mutants resembled *slt-1* single mutants. These results suggest that *mig-10* functions in the *slt-1* axon guidance pathway in AVM.

Synthetic Lethality and Synergistic Axon Guidance Defects in *mig-10; unc-34* Double Mutants

The mammalian Lpd and RIAM proteins bind directly to Ena/VASP proteins through multiple FPPPP motifs [19, 20]. *unc-34* and *mig-10* share similar patterns of axon and cell migration defects, and FPPPP-containing N-terminal and C-terminal fragments of MIG-10 can bind UNC-34 in far Western assays (see Figure S1 in the Supplemental Data available with this article online). To understand the relationship between these two genes, we generated animals with null mutations in both genes. Strikingly, *mig-10; unc-34* double mutants were lethal, unlike either single null mutant (Figure 2). Double mutants arrested with a spectrum of phenotypes between midembryogenesis and the third larval stage. Some embryos failed to undergo morphogenesis, arresting with a mixture of differentiated cells and nonadherent cells (Figure 2A). Others arrested later in development with deformed heads and lumpy cuticles (Figure 2C). These phenotypes are characteristic of defects in epidermal enclosure, a process in midembryogenesis in which epidermal cells surround other embryonic tissues through actin-based motility [29]. The synthetic lethality of *unc-34* and *mig-10* suggests that they have parallel functions in embryonic epithelial morphogenesis.

The AVM axon grows ventrally late in the first larval stage. Although most *mig-10; unc-34* double mutants arrested early in development, ~5% arrested at or after the second larval stage, after AVM guidance was complete. These animals showed severe defects in AVM axon ventral guidance, with more than half of the axons

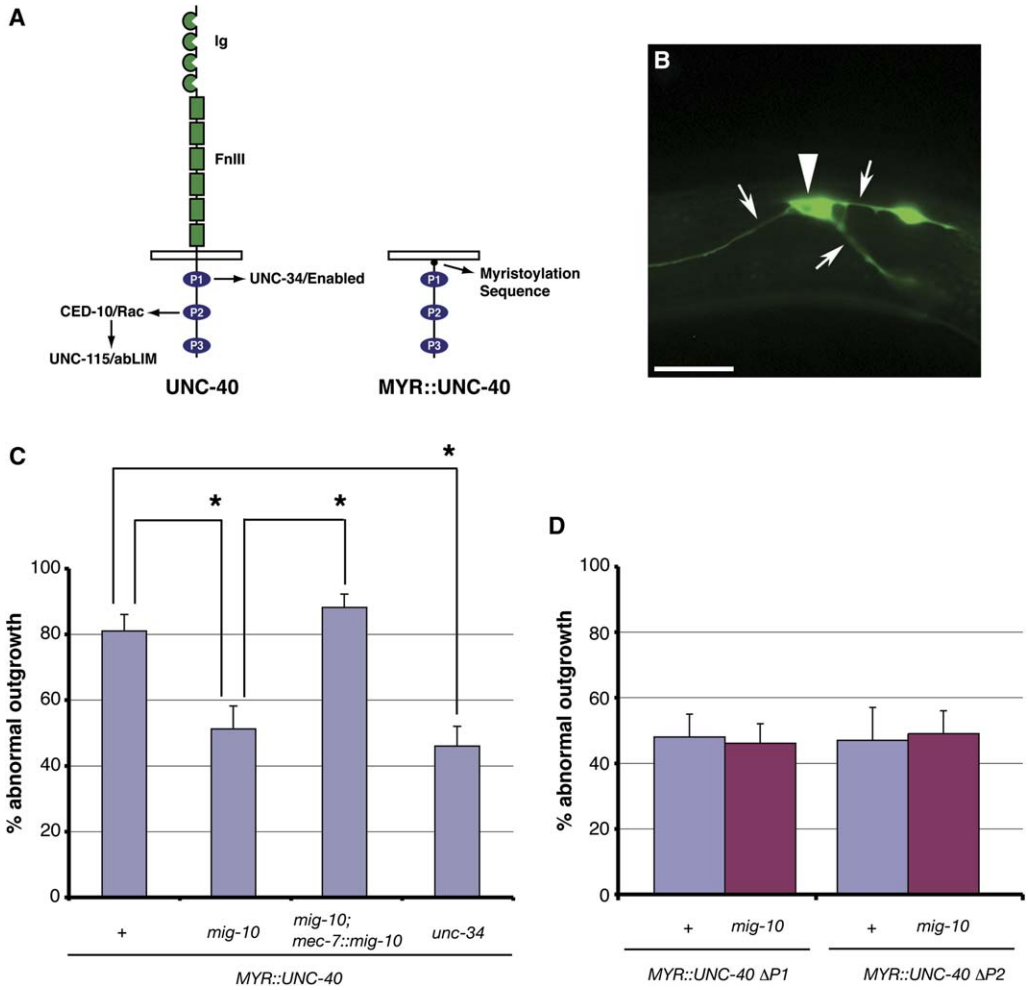

Figure 3. MIG-10 Promotes UNC-40/DCC-Mediated Axon Outgrowth

(A) Schematic diagram of UNC-40 and MYR::UNC-40 showing site of artificial myristoylation, cytoplasmic P1 and P2 motifs, and downstream signaling partners [7].

(B) AVM axon morphology in MYR::UNC-40 animals. Arrowhead indicates cell body; arrows indicate axons. Scale bar equals 10 μm.

(C) Quantitation of defects in MYR::UNC-40-expressing AVM neurons in different mutant backgrounds. Asterisks and brackets represent $p < 0.05$ by t test or Bonferroni t test (in the case of multiple comparisons).

(D) Quantitation of AVM defects in MYR::UNC-40ΔP1 or MYR::UNC-40ΔP2 strains with or without a *mig-10* mutation.

"% abnormal outgrowth" refers to the percentage of animals with misguided AVM axons or excess AVM cell or axon outgrowth (see Figure S2).

affected (Figure 1E). The defect in *mig-10; unc-34* double mutants represents a minimal estimate of their importance in AVM guidance, since some maternal gene product may persist in these animals derived from heterozygous *unc-34*/+ mother [30]. It is possible that the AVM defect in these animals has indirect contributions from *mig-10* effects in other cells. However, the *mig-10* interaction appears specific to *unc-34* and not all actin regulators; for example, *ced-10/Rac; mig-10* double mutants had the mild AVM guidance defects of *mig-10* single mutants (Figure 1E), although *ced-10* has strong genetic interactions with other axon guidance genes [7].

The strongly enhanced axon defect in *mig-10; unc-34* double mutants relative to single mutants suggests that these genes have overlapping functions in AVM axon guidance that are masked by redundancy between them. It is inconsistent with a linear pathway in which either *unc-34* or *mig-10* only regulates the other gene.

mig-10 Promotes UNC-40-Stimulated Axon Outgrowth

Because of Lpd's role in lamellipodial growth, we asked whether *mig-10* has outgrowth-promoting activity in developing neurons. Netrin signaling through DCC receptors stimulates axon outgrowth as well as guidance [31]. AVM neurons expressing MYR::UNC-40, a dominant active form of UNC-40/DCC in which the cytoplasmic domain of UNC-40 is fused to a myristoylation signal, have excessive outgrowth with misguided axons, extra axons, and deformed cell bodies [7] (Figures 3A and 3B and Figure S2). A *mig-10(ct41)* mutation partially suppressed the excessive AVM axon outgrowth caused by MYR::UNC-40 (Figure 3C), suggesting that *mig-10* has outgrowth-promoting activity. The extent of suppression was similar to that caused by null mutations in actin regulators in the netrin pathway such as *unc-34* or *ced-10* [7] (Figure 3C). Expression of a *mig-10*

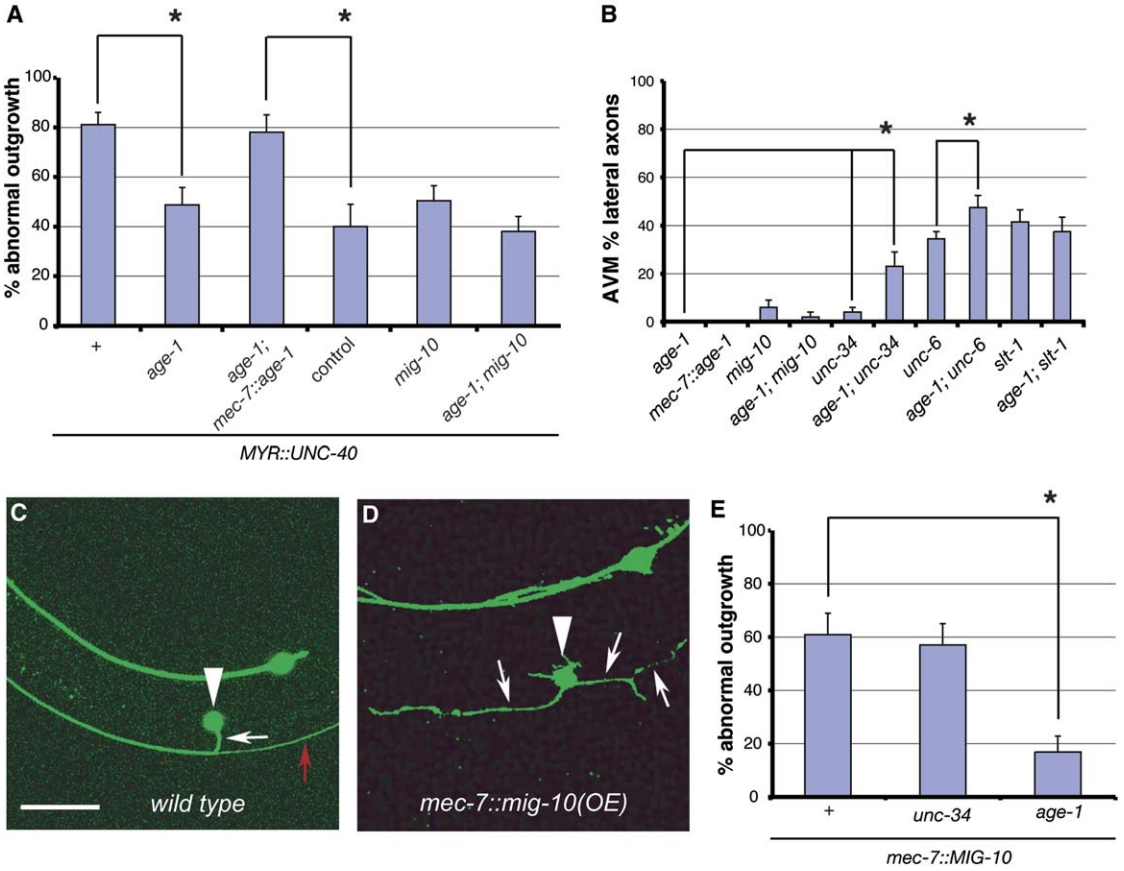

Figure 4. MIG-10 and AGE-1/PI3K Promote Axon Outgrowth

(A) Suppression of MYR::UNC-40 by *age-1* (PI3K) and rescue by expression in AVM. "Control" is nontransgenic siblings of transgenic animals, scored under identical conditions.

(B) Effects of *age-1* and double mutants on AVM ventral axon guidance.

(C and D) AVM axon in (C) wild-type animal and (D) animal overexpressing *mec-7::mig-10*. White arrowheads indicate AVM cell bodies; white arrows indicate AVM axons; red arrow indicates PVM axon. ALM cell body is dorsal and posterior to AVM in both images. Ventral is down and anterior to the left. See Figure S2 for quantitation of defects. Scale bar equals 10 μm.

(E) Suppression of *mec-7::mig-10* overexpression defects by mutation of *age-1* but not *unc-34.*

"% abnormal outgrowth" refers to the percentage of animals with misguided AVM axons or excess AVM cell or axon outgrowth (see Figure S2). Asterisks and brackets represent $p < 0.05$ by t test or Bonferroni t test (in the case of multiple comparisons).

cDNA under the specific *mec-7* promoter restored the exaggerated outgrowth of the MYR::UNC-40 strain (Figure 3C), but the same *mig-10* transgene did not cause outgrowth defects on its own (Figure 1E, Figure S2). These results suggest that MIG-10 can promote axon outgrowth cell autonomously in the AVM neurons.

Two conserved motifs in the UNC-40 cytoplasmic domain called P1 and P2 contribute additively to the outgrowth-promoting activity of MYR::UNC-40 [7] (Figure 3A). Deleting either the P1 motif or the P2 motif from MYR::UNC-40 reduces the severity of the outgrowth defect in AVM neurons; genetic results suggest that P1 is required for activation of UNC-34, and P2 is required for activation of CED-10 [7]. *mig-10* did not suppress all defects caused by P1-deficient or by P2-deficient MYR::UNC-40 transgenes (Figure 3D), but it did change the spectrum of defects in the P1-deficient strain (Figure S2). A possible interpretation of this result is that both the P1 element and the P2 element of UNC-40 contribute to *mig-10* activation.

MIG-10 Acts with AGE-1/PI3K in AVM Outgrowth and Guidance

A potential regulator of MIG-10 suggested by work in other systems is phosphoinositide-3-kinase, or PI3K. During chemotaxis of neutrophils and *Dictyostelium* amoebae, Rac GTPases cooperate with PI3K to define the leading edge of the migrating cell [32, 33]. PI3K stimulates the production of $PI(3,4)P_2$, the lipid ligand of the Lamellipodin PH domain [19]. A null mutation in *age-1,* the *C. elegans* PI3K homolog, significantly suppressed the effects of a MYR::UNC-40 transgene in AVM axons (Figure 4A). This result suggests that *age-1* acts with MYR::UNC-40 to promote AVM outgrowth. Expression of an *age-1* cDNA under the *mec-7* promoter restored the defects to MYR::UNC-40 animals, consistent with an autonomous function of *age-1* in AVM (Figure 4A). *mec-7::age-1* did not cause AVM defects in a wild-type background (Figure 4B). MYR::UNC-40 suppression in *age-1; mig-10* double mutants was comparable to suppression in either *age-1* or *mig-10* alone, consistent with function in a common process.

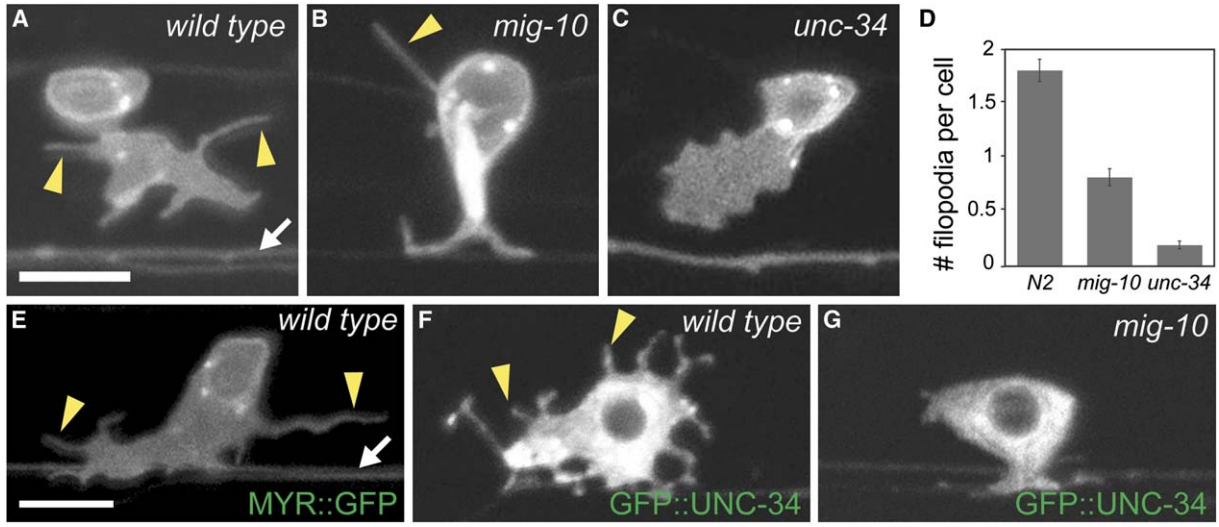

Figure 5. *mig-10* and *unc-34* Stimulate Filopodia Formation

Lateral views of L2-stage animals expressing *unc-86::myrGFP* in the HSN neuron as it grows ventrally in response to netrin. The axon of the PLM neuron is also visible in most panels (white arrow).

(A) Wild-type animal. HSN extends multiple filopodia from its ventrally directed leading edge (arrowheads).

(B) *mig-10* mutant. A filopodium is misplaced to the dorsal cell body (arrowhead).

(C) *unc-34* mutant. HSN extends a leading edge ventrally, but filopodia are not detectable.

(D) Average number of filopodia per HSN. n = 150 cells per genotype.

(E–G) UNC-34-stimulated filopodia formation in HSN growth cones requires MIG-10. HSN growth cones were analyzed in the L2 stage as axons grew ventrally.

(E) Wild-type HSN labeled with *unc-86::myrGFP*. Note filopodia (arrowheads).

(F) GFP::UNC-34 stimulates excessive filopodia formation (arrowheads).

(G) GFP::UNC-34-induced filopodia formation is abolished in *mig-10(ct41)* mutants.

In all images, ventral is down and anterior is to the left. Scale bars equal 5μm. All pictures are confocal micrographs.

To understand the activity of MIG-10 in more detail, we overexpressed *mig-10* in developing neurons and examined the effects on axon morphology. When *mig-10* was overexpressed in AVM neurons by high-copy injection of a *mec-7::mig-10* transgene, it caused defects suggestive of uncontrolled outgrowth and disrupted guidance. Neurons overexpressing MIG-10 had extra axons and deformed cell bodies, an excess outgrowth phenotype similar to the phenotype of neurons expressing MYR::UNC-40 (Figures 4C and 4D, Figure S2). In addition, 41% of MIG-10-overexpressing neurons lacked the characteristic ventral axon in AVM, suggesting a primary axon guidance defect. These defects were not suppressed by null mutations in *unc-34*, but were almost entirely suppressed by an *age-1* null mutation (Figure 4E). These results support the proposal that *age-1* and *mig-10* act in a common process in developing axons.

Loss-of-function mutations in *age-1* had no effect on AVM guidance on their own but had significant effects on ventral guidance in combination with other guidance mutations. In general, *age-1* mutants acted like mild *mig-10* mutants (Figure 4B). *age-1; mig-10* double mutants were similar to *mig-10* single mutants, consistent with action in a common pathway. *age-1; unc-34* double mutants had substantially enhanced defects compared to single mutants, but less severe defects than *mig-10; unc-34* double mutants. *age-1; unc-6* double mutants were slightly more severe than *unc-6* alone and less severe than *mig-10; unc-6* double mutants (Figure 4B). These results suggest that *age-1* is one of several regulators of *mig-10* in AVM guidance.

MIG-10 and UNC-34 Cooperate in Ventral Filopodia Formation Downstream of Netrin

Most studies of axon guidance examine final axon morphology, but the detailed effects of cytoskeletal regulators like MIG-10 and UNC-34 could be more apparent if the actual process of axon guidance is observed. It has not been possible to visualize AVM guidance in real time, but for another neuron, HSN, it is possible to visualize the progress by which the axon navigates to the ventral nerve cord [34]. The HSN neuron grows ventrally toward UNC-6 during the L2 and L3 stages of development. *mig-10* is important for normal HSN ventral guidance (Figure 1C), while *unc-34* has a minor role [7]; both genes also have an earlier function in neuronal polarization prior to axon formation [34].

Filopodia are a prominent feature of neuronal growth cones. Throughout the L2 and L3 stages, the leading edge of HSN has an array of filopodia that extend and retract from the ventral side of the cell body (Figure 5A). *mig-10* mutants had a reduced number of filopodia during HSN ventral guidance, with an average of 0.8 filopodia per cell in the late L2 stage, instead of the 1.8 filopodia seen in wild-type animals (Figures 5B and 5D). Moreover, the occasional filopodia in *mig-10* mutants were often present in abnormal dorsal locations, whereas normal HSN filopodia were always localized to the ventral side of the cell (Figure 5B, arrowhead). This result suggests that MIG-10 promotes filopodia formation and acts with netrin to localize filopodia to the ventral HSN.

unc-34 mutants had a severe defect in filopodia formation during HSN ventral guidance. Virtually all

unc-34 mutant HSNs lacked the spiky filopodial structures seen in all wild-type animals (Figure 5C). At the L2 stage, *unc-34* mutants had an average of only 0.2 filopodia per cell (Figure 5D).

When *unc-34* was overexpressed in HSN neurons, approximately three times as many filopodia were present in developing neurons as were seen in wild-type animals (Figures 5E and 5F). The excessive filopodia caused by *unc-34* overexpression were strongly suppressed by mutations in *mig-10* (Figure 5G). This result suggests that MIG-10 cooperates with UNC-34 to stimulate the formation of filopodia in HSN, while the analysis of AVM indicates that MIG-10 also has separate functions that do not require UNC-34.

Despite the near-complete absence of filopodia, HSN growth cones reached the ventral nerve cord in 92% (n = 105) of *unc-34* animals. This observation indicates that filopodia are largely dispensable for the ventral guidance of HSN axons. It also separates the relative contributions of MIG-10 and UNC-34 in HSN: UNC-34 is central to filopodia formation, but less critical for ventral guidance, whereas MIG-10 is less critical for filopodia formation, but more important for ventral guidance.

Discussion

C. elegans MIG-10 plays roles in both Slit-dependent and netrin-dependent axon guidance pathways. In AVM neurons, MIG-10 promotes repulsion from Slit through the SAX-3/Robo receptor. In HSN neurons, MIG-10 promotes filopodia formation during attractive netrin signaling through the UNC-40 receptor. In addition to its effect on axon guidance, MIG-10 can stimulate cell and axon outgrowth in *C. elegans* neurons, as it can in cultured fibroblasts and T cells [19, 20].

mig-10 activity in developing axons is stimulated by *age-1*, which encodes the lipid kinase PI3K. Lpd has an unusual lipid binding specificity with a strong preference for PI(3,4)P_2 phospholipids, which are products of PI3K. Previous results with pharmacological inhibitors have implicated PI3K in netrin signaling in *Xenopus* neurons [35, 36]; our genetic results provide evidence that PI3K affects axon guidance and outgrowth in vivo and also identify MIG-10 as a potential target of the lipids generated by PI3K. The positive feedback loop between the Rac GTPase and PI3K defined in migrating neutrophils provides one possible pathway from UNC-40/DCC to MIG-10 [33]. In addition, DCC can bind to the focal adhesion kinase (FAK) when phosphorylated by src family kinases [37–39], and FAK kinases can recruit and activate PI3K in other cell types [40]. Mammalian Lpd and RIAM interact with H-, K-, N-, and R-Ras [41], so a Ras-PI3K pathway could provide another mechanism for activation of MIG-10.

Biochemical and genetic results suggest that MIG-10 and UNC-34 (Ena/VASP) have related functions. However, *mig-10* and *unc-34* do not act in a simple linear pathway (Figure S3): each gene has separate functions, the double mutant is lethal, and double mutant escapers have strongly enhanced axon guidance defects. Studies of Lpd and Ena/VASP proteins in mammalian cells also suggest that they have distinct functions, although the experiments have not been conducted in the same cell types. Lpd is required for lamellipodia formation in melanoma cells [19]. Ena/VASP function is required for filopodia formation in fibroblast and neurons, but cells that lack Ena/VASP function can still form lamellipodia, though the dynamics are different [42, 13]. In addition to its synthetic lethality with *mig-10*, *C. elegans unc-34* also has synthetic lethal interactions with the actin-regulatory proteins of the Wasp and WAVE complexes [30]. These results suggest that these proteins belong to a broad network of cytoskeletal regulators with partly overlapping functions. Interestingly, WASP, WAVE, Ena, Lpd, and other actin-regulatory proteins can be copurified in a common complex from the mammalian brain [43].

Ena/VASP proteins are strongly implicated in filopodia formation [13, 17]. Our results support the importance of this interaction for UNC-34 and also show that MIG-10 enhances filopodia formation in vivo. Because filopodia are a general feature of growth cones, they have been thought to be critical for axon guidance. The sole *C. elegans* Ena/VASP protein UNC-34 is essential for generating filopodia downstream of netrin but is largely dispensable for HSN guidance toward the ventral nerve cord. Thus growth cone guidance in vivo can be accurate without many filopodia, perhaps through the alternative motility mechanisms stimulated by MIG-10 and by Rac pathways [7]. Although filopodia represent an elegant extended structure for exploring broad regions and evaluating shallow gradients with minimal cytoskeletal commitment, they may not be essential when guidance cues are relatively unambiguous or when the migration distances are relatively short.

We suggest that MIG-10 has two signaling modes, one in which it acts mainly with UNC-34 to organize filopodia, and one in which it acts mainly with AGE-1-dependent phospholipids to stimulate lamellipodial outgrowth (Figure S3). At this point, we do not know the exact rules for recruitment and activation of these molecules, but the genetic results show clear differences between the ways that MIG-10 functions even within a single neuron. The cooperative action of lipid-modulating enzymes, actin regulators, and multifunctional linkers such as MIG-10 provides multiple points of contact between specific guidance receptors and the shared signaling components in a developing neuron.

Experimental Procedures

Strains

Nematodes were cultivated according to standard protocols and maintained at 20ºC [44]. The following mutations and transgenes were used: LGI, *zdIs5[mec-4::gfp, lin-15(+)]*, *kyIs170[srh-220::gfp, lin-15(+)]*; LGII, *age-1(mg44)*; LGIII, *mig-10(ct41)*; LGIV, *zdIs1[ceh-23::GFP*, *lin-15(+)]*, *zdIs4[mec-4::gfp, lin-15(+)]*, *kyIs262[unc-86::myr GFP, odr-1dsred]*; LGV, *unc-34(gm104)*; LGX, *unc-6(ev400), slt-1(eh15), sax-3(ky123)*. Transgenes maintained as extrachromosomal arrays included: *cyEx21[mec-7::mig-10a, odr-1dsred]*, *kyEx456[unc-86::myr::unc-40, str-1::gfp]*, *kyEx637[unc-86::myr::unc-40(ΔP2), odr-1::dsred]*, *kyEx639[unc-86::myr::unc-40(ΔP1), odr-1::dsred]*, *kyEx710 [unc-86::GFP::unc-34, odr-1dsred],* and *kyEx1094[mec-7::age-1, odr-1dsred]*.

Transgenes used to characterize axon guidance defects in Figure 1 were *kyIs262* (HSN), *zdIs5* (AVM), *kyIs170* (ADL), and *zdIs1* (CAN).

Germline transformation of *C. elegans* was performed by standard techniques [44]. The *mec-7::mig-10a* and *mec-7::age-1* overexpressing lines were injected at 100 ng/μl along with the coinjection marker *odr-1::dsred* at 70 ng/μl. Transgenic lines were maintained by following *odr-1::dsred* fluorescence with a Zeiss M^{2}BIO imaging

system. For the *mig-10* and *age-1* cell-autonomy experiments, two independent transgenic lines with similar properties were analyzed; the data shown are from one line. *kyEx456, kyEx637*, and *kyEx639* transgenes have been described previously [7]. Some mutant strains were kindly provided by Gian Garriga at Berkeley or Theresa Stiernagle of the *Caenorhabditis* Genetics Center.

Microscopy

Axonal processes of AVM neurons were visualized with the integrated *mec-4::gfp* transgene *zdIs5* in young adult animals, except for *mig-10; unc-34* doubles, which were analyzed at the L2-L3 stage. The observer was not blind to the genotype. Animals were placed on 5% Noble Agar pads in M9 buffer containing 10 mM sodium azide and examined with a Plan-NEOFLUAR 40× objective on a Zeiss Axioplan 2. Arrested *mig-10; unc-34* double mutants were picked from agar plates where embryos laid from *mig-10; unc-34*/+ parents had developed for 48 hr. Arrested animals were analyzed with a Plan-APOCHROMAT 100× objective with Nomarski optics. Images for axons and body morphology were captured with a SPOT camera (RT Slider Diagnostic Instruments, Inc.). All pictures of HSN are projections of Z-stacks captured on a BioRad MRC1024 confocal with a 63× oil objective.

Developmental Analysis of HSN Neurons

Embryos were released from gravid adults by standard techniques [44], then synchronized by overnight starvation in M9 buffer. Animals were then fed and grown at 25ºC until the late L2 stage [34]. In wild-type animals, this occurred ~20 hr after feeding; in *mig-10* and *unc-34* animals, this occurred ~25 hr after feeding. Populations were examined by standard epifluorescence on a Zeiss Axioplan2 with a 63× oil objective.

Molecular Biology

mec-7::mig-10a was generated by cloning the *mig-10a* cDNA into KpnI and XhoI sites of the pPD96.41 vector containing the *mec-7* promoter, and *mec-7::age-1* was generated by cloning *age-1* cDNA into BglII and Nhe1 sites of the pPD96.41 vector. pPD96.41 was a gift of Andrew Fire (Stanford University). To generate *unc-86::GFP::unc-34*, an *unc-34* cDNA was amplified by PCR and inserted at the 3′ end of GFP in a pPD95.75 vector containing a 5 kb fragment of the *unc-86* promoter [45] between SpnI and SalI sites. The *unc-34* cDNA was provided by Tim Yu and the *mig-10a* cDNA was provided by Yuji Kohara (National Institute of Genetics, Japan).

Supplemental Data

Supplemental Data include three figures and Supplemental Experimental Procedures and can be found with this article online at http://www.current-biology.com/cgi/content/full/16/9/854/DC1/.

Acknowledgments

We thank Zemer Gitai, Tim Yu, and Joe Hao for discussion and insights, Theresa Stiernagle of the *Caenorhabditis* Genetic Center, Gian Garriga, Yuji Kohara, Tim Yu, and Andrew Fire for strains and plasmids, and Chris Quinn and Bill Wadsworth for sharing results prior to publication. This work was supported by an American Cancer Society Postdoctoral Fellowship to C.C., a National Science Foundation Predoctoral Fellowship to C.E.A., NIH grant GM68678 to F.B.G., and by the Howard Hughes Medical Institute. C.I.B. is an Investigator of the Howard Hughes Medical Institute.

Received: November 13, 2005
Revised: March 19, 2006
Accepted: March 24, 2006
Published online: April 13, 2006

References

1. Dickson, B.J. (2002). Molecular mechanisms of axon guidance. Science *298*, 1959–1964.
2. Tessier-Lavigne, M., and Goodman, C.S. (1996). The molecular biology of axon guidance. Science *274*, 1123–1133.
3. Yu, T.W., and Bargmann, C.I. (2001). Dynamic regulation of axon guidance. Nat. Neurosci. *4*, 1169–1176.
4. Strasser, G.A., Rahim, N.A., VanderWaal, K.E., Gertler, F.B., and Lanier, L.M. (2004). Arp2/3 is a negative regulator of growth cone translocation. Neuron *43*, 81–94.
5. Bashaw, G.J., Kidd, T., Murray, D., Pawson, T., and Goodman, C.S. (2000). Repulsive axon guidance: Abelson and Enabled play opposing roles downstream of the roundabout receptor. Cell *101*, 703–715.
6. Fan, X., Labrador, J.P., Hing, H., and Bashaw, G.J. (2003). Slit stimulation recruits Dock and Pak to the roundabout receptor and increases Rac activity to regulate axon repulsion at the CNS midline. Neuron *40*, 113–127.
7. Gitai, Z., Yu, T.W., Lundquist, E.A., Tessier-Lavigne, M., and Bargmann, C.I. (2003). The netrin receptor UNC-40/DCC stimulates axon attraction and outgrowth through enabled and, in parallel, Rac and UNC-115/AbLIM. Neuron *37*, 53–65.
8. Krugmann, S., Jordens, I., Gevaert, K., Driessens, M., Vandekerckhove, J., and Hall, A. (2001). Cdc42 induces filopodia by promoting the formation of an IRSp53:Mena complex. Curr. Biol. *11*, 1645–1655.
9. Han, Y.H., Chung, C.Y., Wessels, D., Stephens, S., Titus, M.A., Soll, D.R., and Firtel, R.A. (2002). Requirement of a vasodilator-stimulated phosphoprotein family member for cell adhesion, the formation of filopodia, and chemotaxis in *Dictyostelium*. J. Biol. Chem. *277*, 49877–49887.
10. Barzik, M., Kotova, T.I., Higgs, H.N., Hazelwood, L., Hanein, D., Gertler, F.B., and Schafer, D.A. (2005). Ena/VASP proteins enhance actin polymerization in the presence of barbed end capping proteins. J. Biol. Chem. *280*, 28653–28662.
11. Yu, T.W., Hao, J.C., Lim, W., Tessier-Lavigne, M., and Bargmann, C.I. (2002). Shared receptors in axon guidance: SAX-3/Robo signals via UNC-34/Enabled and a Netrin-independent UNC-40/DCC function. Nat. Neurosci. *5*, 1147–1154.
12. Bear, J.E., Svitkina, T.M., Krause, M., Schafer, D.A., Loureiro, J.J., Strasser, G.A., Maly, I.V., Chaga, O.Y., Cooper, J.A., Borisy, G.G., et al. (2002). Antagonism between Ena/VASP proteins and actin filament capping regulates fibroblast motility. Cell *109*, 509–521.
13. Lebrand, C., Dent, E.W., Strasser, G.A., Lanier, L.M., Krause, M., Svitkina, T.M., Borisy, G.G., and Gertler, F.B. (2004). Critical role of Ena/VASP proteins for filopodia formation in neurons and in function downstream of netrin-1. Neuron *42*, 37–49.
14. Huang, X., Cheng, H.J., Tessier-Lavigne, M., and Jin, Y. (2002). MAX-1, a novel PH/MyTH4/FERM domain cytoplasmic protein implicated in netrin-mediated axon repulsion. Neuron *34*, 563–576.
15. Niebuhr, K., Ebel, F., Frank, R., Reinhard, M., Domann, E., Carl, U.D., Walter, U., Gertler, F.B., Wehland, J., and Chakraborty, T. (1997). A novel proline-rich motif present in ActA of *Listeria monocytogenes* and cytoskeletal proteins is the ligand for the EVH1 domain, a protein module present in the Ena/VASP family. EMBO J. *16*, 5433–5444.
16. Gertler, F.B., Niebuhr, K., Reinhard, M., Wehland, J., and Soriano, P. (1996). Mena, a relative of VASP and *Drosophila* Enabled, is implicated in the control of microfilament dynamics. Cell *87*, 227–239.
17. Krause, M., Dent, E.W., Bear, J.E., Loureiro, J.J., and Gertler, F.B. (2003). ENA/VASP proteins: regulators of the actin cytoskeleton and cell migration. Annu. Rev. Cell Dev. Biol. *19*, 541–564.
18. Zimmermann, J., Labudde, D., Jarchau, T., Walter, U., Oschkinat, H., and Ball, L.J. (2002). Relaxation, equilibrium oligomerization, and molecular symmetry of the VASP (336–380) EVH2 tetramer. Biochemistry *41*, 11143–11151.
19. Krause, M., Leslie, J.D., Stewart, M., Lafuente, E.M., Valderrama, F., Jagannathan, R., Strasser, G.A., Rubinson, D.A., Liu, H., Way, M., et al. (2004). Lamellipodin, an Ena/VASP ligand, is implicated in the regulation of lamellipodial dynamics. Dev. Cell *7*, 571–583.
20. Lafuente, E.M., van Puijenbroek, A.A., Krause, M., Carman, C.V., Freeman, G.J., Berezovskaya, A., Constantine, E., Springer, T.A., Gertler, F.B., and Boussiotis, V.A. (2004). RIAM, an Ena/VASP and Profilin ligand, interacts with Rap1-GTP and mediates Rap1-induced adhesion. Dev. Cell *7*, 585–595.
21. Manser, J., Roonprapunt, C., and Margolis, B. (1997). *C. elegans* cell migration gene *mig-10* shares similarities with a family of

SH2 domain proteins and acts cell nonautonomously in excretory canal development. Dev. Biol. *184*, 150–164.

22. Forrester, W.C., and Garriga, G. (1997). Genes necessary for *C. elegans* cell and growth cone migrations. Development *124*, 1831–1843.
23. Hao, J.C. (2003). Genetic analysis of axon guidance and branching in *C. elegans*. PhD thesis, University of California, San Francisco, San Francisco, California.
24. Hamelin, M., Scott, I.M., Way, J.C., and Culotti, J.G. (1992). The *mec-7* beta-tubulin gene of *Caenorhabditis elegans* is expressed primarily in the touch receptor neurons. EMBO J. *11*, 2885–2893.
25. Ishii, N., Wadsworth, W.G., Stern, B.D., Culotti, J.G., and Hedgecock, E.M. (1992). UNC-6, a laminin-related protein, guides cell and pioneer axon migrations in *C. elegans*. Neuron *9*, 873–881.
26. Chan, S.S., Zheng, H., Su, M.W., Wilk, R., Killeen, M.T., Hedgecock, E.M., and Culotti, J.G. (1996). UNC-40, a *C. elegans* homolog of DCC (Deleted in Colorectal Cancer), is required in motile cells responding to UNC-6 netrin cues. Cell *87*, 187–195.
27. Hao, J.C., Yu, T.W., Fujisawa, K., Culotti, J.G., Gengyo-Ando, K., Mitani, S., Moulder, G., Barstead, R., Tessier-Lavigne, M., and Bargmann, C.I. (2001). *C. elegans* slit acts in midline, dorsal-ventral, and anterior-posterior guidance via the SAX-3/Robo receptor. Neuron *32*, 25–38.
28. Chang, C., Yu, T.W., Bargmann, C.I., and Tessier-Lavigne, M. (2004). Inhibition of netrin-mediated axon attraction by a receptor protein tyrosine phosphatase. Science *305*, 103–106.
29. Williams-Masson, E.M., Malik, A.N., and Hardin, J. (1997). An actin-mediated two-step mechanism is required for ventral enclosure of the *C. elegans* hypodermis. Development *124*, 2889–2901.
30. Withee, J., Galligan, B., Hawkins, N., and Garriga, G. (2004). *Caenorhabditis elegans* WASP and Ena/VASP proteins play compensatory roles in morphogenesis and neuronal cell migration. Genetics *167*, 1165–1176.
31. Graef, I.A., Wang, F., Charron, F., Chen, L., Neilson, J., Tessier-Lavigne, M., and Crabtree, G.R. (2003). Neurotrophins and netrins require calcineurin/NFAT signaling to stimulate outgrowth of embryonic axons. Cell *113*, 657–670.
32. Park, K.C., Rivero, F., Meili, R., Lee, S., Apone, F., and Firtel, R.A. (2004). Rac regulation of chemotaxis and morphogenesis in *Dictyostelium*. EMBO J. *23*, 4177–4189.
33. Weiner, O.D., Neilsen, P.O., Prestwich, G.D., Kirschner, M.W., Cantley, L.C., and Bourne, H.R. (2002). A PtdInsP(3)- and Rho GTPase-mediated positive feedback loop regulates neutrophil polarity. Nat. Cell Biol. *4*, 509–513.
34. Adler, C.E., Fetter, R.D., and Bargmann, C.I. (2006). UNC-6/Netrin induces neuronal asymmetry and defines the site of axon formation. Nat. Neurosci. *9*, 511–518.
35. Campbell, D.S., and Holt, C.E. (2001). Chemotropic responses of retinal growth cones mediated by rapid local protein synthesis and degradation. Neuron *32*, 1013–1026.
36. Ming, G., Song, H., Berninger, B., Inagaki, N., Tessier-Lavigne, M., and Poo, M. (1999). Phospholipase C-gamma and phosphoinositide 3-kinase mediate cytoplasmic signaling in nerve growth cone guidance. Neuron *23*, 139–148.
37. Li, W., Lee, J., Vikis, H.G., Lee, S.H., Liu, G., Aurandt, J., Shen, T.L., Fearon, E.R., Guan, J.L., Han, M., et al. (2004). Activation of FAK and Src are receptor-proximal events required for netrin signaling. Nat. Neurosci. *7*, 1213–1221.
38. Liu, G., Beggs, H., Jurgensen, C., Park, H.T., Tang, H., Gorski, J., Jones, K.R., Reichardt, L.F., Wu, J., and Rao, Y. (2004). Netrin requires focal adhesion kinase and Src family kinases for axon outgrowth and attraction. Nat. Neurosci. *7*, 1222–1232.
39. Meriane, M., Tcherkezian, J., Webber, C.A., Danek, E.I., Triki, I., McFarlane, S., Bloch-Gallego, E., and Lamarche-Vane, N. (2004). Phosphorylation of DCC by Fyn mediates Netrin-1 signaling in growth cone guidance. J. Cell Biol. *167*, 687–698.
40. Hanks, S.K., Ryzhova, L., Shin, N.Y., and Brabek, J. (2003). Focal adhesion kinase signaling activities and their implications in the control of cell survival and motility. Front. Biosci. *8*, 982–996.
41. Rodriguez-Viciana, P., Sabatier, C., and McCormick, F. (2004). Signaling specificity by Ras family GTPases is determined by the full spectrum of effectors they regulate. Mol. Cell. Biol. *24*, 4943–4954.
42. Bear, J.E., Loureiro, J.J., Libova, I., Fassler, R., Wehland, J., and Gertler, F.B. (2000). Negative regulation of fibroblast motility by Ena/VASP proteins. Cell *101*, 717–728.
43. Salazar, M.A., Kwiatkowski, A.V., Pellegrini, L., Cestra, G., Butler, M.H., Rossman, K.L., Serna, D.M., Sondek, J., Gertler, F.B., and De Camilli, P. (2003). Tuba, a novel protein containing bin/amphiphysin/Rvs and Dbl homology domains, links dynamin to regulation of the actin cytoskeleton. J. Biol. Chem. *278*, 49031–49043.
44. Epstein, H.F., and Shakes, D.C. (1995). *Caenorhabditis elegans*: Modern Biological Analysis of an Organism (New York: Academic Press).
45. Baumeister, R., Liu, Y., and Ruvkun, G. (1996). Lineage-specific regulators couple cell lineage asymmetry to the transcription of the *Caenorhabditis elegans* POU gene *unc-86* during neurogenesis. Genes Dev. *10*, 1395–1410.